Sequence-Specific Polyampholyte Phase Separation in Membraneless Organelles

Yi-Hsuan Lin,[1,2] Julie D. Forman-Kay,[2,1] and Hue Sun Chan[1,3,*]

[1]*Department of Biochemistry, University of Toronto, 1 King's College Circle, Toronto, Ontario M5S 1A8, Canada*
[2]*Molecular Structure and Function Program, Hospital for Sick Children, 686 Bay Street, Toronto, Ontario M5G 0A4, Canada*
[3]*Department of Molecular Genetics, University of Toronto, Toronto, 1 King's College Circle, Toronto, Ontario M5S 1A8, Canada*

Liquid-liquid phase separation of charge- and/or aromatic-enriched intrinsically disordered proteins (IDPs) is critical in the biological function of membraneless organelles. Much of the physics of this recent discovery remains to be elucidated. Here, we present a theory in the random phase approximation to account for electrostatic effects in polyampholyte phase separations, yielding predictions consistent with recent experiments on the IDP Ddx4. The theory is applicable to any charge pattern and thus provides a general analytical framework for studying sequence dependence of IDP phase separation.

The biological function of proteins has long been associated with their ordered, often globular, structures. It is now clear, however, that many critical cellular functions—in signaling and cell-cycle regulation in particular—are performed by intrinsically disordered proteins (IDPs) that lack a unique fold. IDPs are depleted in hydrophobic but are enriched in charged and polar amino acids [1–5]. Many IDPs are polyampholytes with both positively and negatively charged monomers [6,7]. Recently, some polyampholytic IDPs were found to function not only as individual molecules but also collectively by undergoing phase separation on a mesoscopic length scale to form condensed liquid-phase nonamyloidogenic IDP-rich droplets that may encompass ribonucleic acid (RNA) and other biomolecules [8–12]. This phase behavior is the basis of functional membraneless organelles in the cell. Without a membrane, these organelles can respond rapidly to environmental stimuli. They are critical for cellular integrity, homeostasis [12,13], and the spatial-temporal control of gene regulation and cell growth [11,12,14–17]. In view of the biological and biomedical importance of this newly discovered phenomenon, insights into its physics would be valuable.

In line with charge effects on the size of individual IDP molecules [18–21], electrostatics figured prominently in computational [22] and experimental [12,23] analysis of IDP phase separation. Polymer theory emphasized the sensitivity of polyampholyte phase behavior to charge pattern [6,7], but only a few simple patterns were considered [24–26]. No systematic approach has been put forth to apply those ideas to understanding phase behaviors of genetically coded proteins. Inasmuch as IDP phase separation is concerned, the theoretical discussion to date remains at the mean-field level [11,12,15,17], which precludes sequence dependence to be addressed. In this Letter, we take a step forward by developing an analytical theory for sequence-specific electrostatics in polyampholyte phase separation, aiming to synergize theory and experiment and lay the groundwork for further theoretical advances.

While our theory is applicable to any charge sequence, an impetus for our effort was the recent experiments on the RNA helicase Ddx4, the N terminal of which is an IDP, that can undergo *in vitro* and in cell phase separation under ambient conditions [12]. Ddx4 is essential for the assembly and maintenance of the related nuage in mammals, P granules in worms, and pole plasm and polar granules in flies [12,27]. The wild-type sequence of the residue 1–236 N-terminal disordered region of Ddx4 (termed Ddx4^{N1}) may be seen by sliding-window averaging as a series of alternating charge blocks abounding with negatively charged aspartic (D) and glutamic (E) acids and positively charged arginines (R) and lysines (K) [12]. In the absence of this block-charge pattern, a charge-scrambled mutant Ddx4^{N1}CS does not phase separate [12]. Thus, the sequence-specific charge pattern—not the total positive and total negative charges *per se*—is crucial for Ddx4 phase behavior.

Since it is challenging to synthesize nonbiological polyampholytes with specific charge patterns [7], theories have focused on the quenched ensemble average of random sequences [6,28] or limited to diblock [24] or, at most, four-block charge patterns [25,26]. In contrast, a high diversity of protein sequences is readily synthesized by the cellular machinery. In view of this expanded experimental horizon, the availability of a large repertoire of IDP sequences for phase separation studies is foreseeable with the new physics that is likely to ensue. With this in mind, we present below a random phase approximation (RPA) theory [24,28–32] for any charge pattern and, as an example, apply our theory to elucidate Ddx4 phase behavior.

As in prior applications of the RPA, the particle density in our theory is assumed to be rather homogeneous to permit an approximate account based solely on two-body correlations of density fluctuation [29]. Electrostatic free energy is similarly approximated by a Gaussian integral over charge fluctuations. Other limitations of the RPA, such as in its treatment of short-range electrostatic interactions, are well documented (e.g., Refs. [29,30]). Approximations

notwithstanding, the RPA represents a significant improvement, especially amidst the current interest in IDP phase separation [15,17], over Debye-Hückel theory for biological coacervation [33] in that the RPA embodies chain connectivity [29,30] and hence allows for an explicit account of the charge pattern along the chain sequence [24,28].

Based on previous approaches [24,28], our theory is for a system of aqueous polyampholytes, small counterions, and salt. In contrast to self-repelling, strongly charged polyelectrolytes that necessitate a modified RPA [30,34], we focus on polyampholytes that are nearly neutral, i.e., with approximately equal numbers of acidic and basic residues (e.g., Ddx4^{N1} and Ddx4^{N1}CS). Each polyampholyte consists of N monomers (amino acid residues) with charges $\{\sigma_i\} = \{\sigma_1, \sigma_2, ..., \sigma_N\}$, where σ_i is in units of the electronic charge e. The counterions and salt are monovalent in this formulation. The densities of monomers, counterions, and salt are denoted, respectively, by ρ_m, ρ_c, and ρ_s. The number of monovalent counterions is taken to be equal to the net charge of polyampholytes, viz., $\rho_c = \rho_m |\sum_i \sigma_i|/N$. The free energy F of our system per volume V in units of $k_B T$ is

$$f \equiv \frac{F}{V k_B T} = -s + f_{el}, \qquad (1)$$

where k_B is Boltzmann's constant and T is absolute temperature, s is the entropic contribution, and f_{el} accounts for electrostatic interactions. As IDPs have few hydrophobic residues, as a first step in our development, we assume that electrostatics is the dominant enthalpic contribution while neglecting presumably weaker short-range attractive forces. For simplicity, all monomers of the polyampholytes as well as the counterions and salt ions are taken to be of an equal size, with length scale a. The entropic term that accounts for excluded volume follows directly from Flory-Huggins (FH) theory [35–37]:

$$-sa^3 = \frac{\phi_m}{N}\ln(\phi_m) + \phi_c \ln(\phi_c) + 2\phi_s \ln(\phi_s)$$
$$+ (1 - \phi_m - \phi_c - 2\phi_s)\ln(1 - \phi_m - \phi_c - 2\phi_s), \qquad (2)$$

where ϕ_m, ϕ_c, and ϕ_s are, respectively, the volume ratios $\rho_m a^3$, $\rho_c a^3$, and $\rho_s a^3$. A uniform, phase-independent ϕ_s is assumed here for simplicity, as previous work suggested that the change in salt concentration is insignificant upon biological coacervation [33]. The f_{el} term for electrostatics is computed by the RPA [28,30–32]:

$$f_{el} = \frac{1}{2}\int \frac{d^3k}{(2\pi)^3}\{\ln[\det(1 + \hat{G}_k \hat{U}_k)] - \text{Tr}(\hat{\rho}\hat{U}_k)\}, \qquad (3)$$

where $\hat{G}_k$, $\hat{U}_k$, and $\hat{\rho}$ are $(N + 2) \times (N + 2)$ matrices. The logarithmic term containing $\hat{G}_k$ for a basic, "bare" density correlation without electrostatic effects and $\hat{U}_k$ for Coulombic interactions, both defined for the reciprocal k space, is a result of standard Gaussian integrations in RPA

theory. The second trace term subtracts the self-electrostatic energy for all charge densities to eliminate the unphysical divergence of the first term for $k \to \infty$ [28,31,32]. The density matrix

$$\hat{\rho} = \begin{pmatrix} (\rho_m/N)\hat{I}_N & 0 \\ 0 & \hat{\rho}_I \end{pmatrix} \qquad (4)$$

is a diagonal matrix, with $\hat{I}_N$ being the N-dimensional identity and $\hat{\rho}_I$ a 2×2 diagonal matrix for the positive and negative monovalent ions, namely, $((\hat{\rho}_I)_{11}, (\hat{\rho}_I)_{22}) = (\rho_s + \rho_c, \rho_s)$ or $(\rho_s, \rho_s + \rho_c)$ when the net polyampholyte charge is, respectively, negative or positive.

The bare correlation matrix $\hat{G}_k$ combines the monomer-monomer correlation for a Gaussian chain and the density matrix for the small monovalent ions:

$$\hat{G}_k = \begin{pmatrix} (\rho_m/N)\hat{G}_M(k) & 0 \\ 0 & \hat{\rho}_I \end{pmatrix}, \qquad (5)$$

where $\hat{G}_M(k)$ is the $N \times N$ matrix for Gaussian chains, with elements $\hat{G}_M(k)_{ij} = \exp[-(ka)^2|i - j|/6]$ [38].

The interaction matrix $\hat{U}_k$ is the Fourier transform of the Coulomb potential with a short-range physical cutoff on the scale of monomer size, $U(r) = l_B(1 - e^{-r/a})/r$, which, in k space, becomes [31,32]

$$\hat{U}_k = \frac{4\pi l_B}{k^2[1 + (ka)^2]}|q\rangle\langle q| \equiv \lambda(k)|q\rangle\langle q|. \qquad (6)$$

Here, $l_B = e^2/(4\pi\epsilon_0\epsilon k_B T)$ is the Bjerrum length, ϵ_0 is the vacuum permittivity, ϵ is the dielectric constant, $|q\rangle$ is the column vector for the charges of the monomers and the monovalent ions, and $\langle q| \equiv |q\rangle^T$ is the transposed row vector, with components $q_i = \sigma_i$ for $1 \le i \le N$, $q_{N+1} = 1$, and $q_{N+2} = -1$.

The determinant in Eq. (3) can now be simplified as

$$\det(1 + \hat{G}_k\hat{U}_k) = 1 + \lambda(k)\langle q|\hat{G}_k|q\rangle \qquad (7)$$

by Sylvester's identity [29]. For the analysis below, we define a reduced temperature $T^* \equiv a/l_B = 4\pi\epsilon_0\epsilon k_B T a/e^2$.

We first consider a simple salt-free ($\rho_s = 0$) solution of polyampholytes consisting of n alternating charge blocks (labeled by $\alpha, \beta = 1, 2, ..., n$), each with one charge per $1/\sigma$ monomer, i.e., $\sigma_\alpha^{block} = (-1)^{\alpha-1}\sigma$ and length $L = N/n$ [28]. The correlation matrix $\hat{G}_M(k)$ in this case is an $n \times n$ matrix for the blocks, with

$$\hat{G}_M^{block}(k)_{\alpha\beta} = \begin{cases} \dfrac{1+\zeta}{1-\zeta}L\sigma - \dfrac{2\zeta(1 - \zeta^{L\sigma})}{(1-\zeta)^2}, & \alpha = \beta, \\[2ex] \dfrac{\zeta^{(|\alpha-\beta|-1)L\sigma+1}}{(1-\zeta)^2}(1 - \zeta^{L\sigma})^2, & \alpha \neq \beta, \end{cases} \qquad (8)$$

where $\zeta = \exp[-(ka)^2/(6\sigma)]$. Results for block polyampholytes that are neutral (n even, $\rho_c = 0$; see Fig. 1)
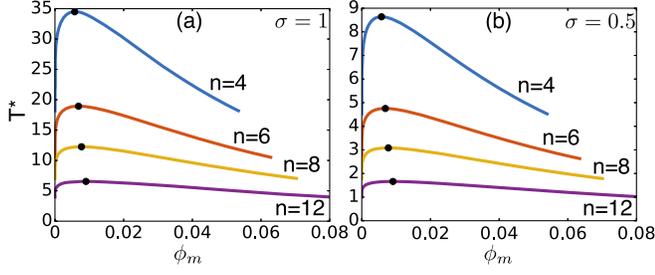
FIG. 1.   Phase diagrams of $N = 240$ salt-free polyampholytes with 4, 6, 8, and 12 alternating charge blocks of $\sigma_\alpha^{block} = (-1)^{\alpha-1}\sigma$; ϕ_m and T^* are, respectively, the dimensionless polymer volume ratio and the temperature (see the text). A dilute and a condensed phase exist, respectively, above and below each phase-boundary curve. (a) $\sigma = 1$. (b) $\sigma = 0.5$. The black dots are the critical points (ϕ_{cr}, T^*_{cr}). Polyampholytes with fewer blocks and a stronger σ phase separate at a higher T^*.

FIG. 2.   (a) The Ddx4^{N1} (top panel) and Ddx4^{N1}CS (bottom panel) amino acid sequences. Positively ($+$) and negatively ($-$) charged (basic and acidic) and aromatic residues are highlighted, respectively, in red, turquoise, and yellow. (b) Charge patterns of the sequences ($+$, red; $-$, blue) indicate that the charges exhibit more blocklike properties (repeated red or repeated blue) and are less evenly dispersed in Ddx4^{N1} than in Ddx4^{N1}CS (cf. Fig. 6A of Ref. [12]). (c) Theoretical phase diagrams computed by Eq. (3) under salt-free conditions. (d) Ddx4^{N1} phase diagrams [Eq. (3)] for different monovalent salt (NaCl) concentrations.

indicate that, when N is fixed, the tendency to phase separate decreases (i.e., requires a lower T^*) with an increasing n [Fig. 1(a)]. This predicted behavior offers insights into Ddx4 behavior (see below) and is consistent with theoretical findings from a charged hard-sphere chain model [26] and grand canonical Monte Carlo simulations [25]. While a stronger σ leads generally to a higher phase separation T^* (and thus a higher critical temperature T^*_{cr}), the critical concentration ϕ_{cr} is determined mainly by the block number n, and barely by σ [cf. curves for the same n in Figs. 1(a) and 1(b)]. When an increasing n arrives at a strictly alternating polyampholyte with $\sigma = 1/L$, the contribution of $\hat{G}_M^{block}(k)$ in $\langle q|\hat{G}_k|q\rangle$,

$$\frac{1}{N}\langle\sigma|\hat{G}_M^{block}(k)|\sigma\rangle = \frac{1-\zeta}{1+\zeta}\sigma + \frac{1}{N}\frac{2\zeta[1-(-1)^n\zeta^{N\sigma}]}{(1+\zeta)^2}, \quad (9)$$

contains the second $O(1/N)$ term, which diminishes as $N \to \infty$. In that limit, the first term leads to $f_{el} \propto \phi_m^2$ after integration, defining an effective FH parameter $\chi \propto \sigma^{3/2}/T^{*2}$ for electrostatics [28]. When N is finite, the second term enhances phase separation, resulting in a ϕ_{cr} much smaller than the $\phi_{cr} = 1/\sqrt{N}$ predicted by FH theory. For example, for $N = 240$, $\sigma = 1$ and 0.5, $\phi_{cr} = 0.0213$ and 0.0192, respectively. Both ϕ_{cr} values are much smaller than the FH value of $1/\sqrt{240} = 0.06$.

We now apply the full theory to Ddx4 by considering the exact Ddx4^{N1} and charged scrambled Ddx4^{N1}CS sequences [Fig. 2(a)]. There are 32 positively and 36 negatively charged residues in either sequence [Fig. 2(b)], the two polyampholytes are thus nearly neutral [12]. We assign $\sigma_i = 1$ to each of the 28 R and 4 K residues, $\sigma_i = -1$ to each of the 18 D and 18 E residues, and $\sigma_i = 0$ to all other residues. We then substitute these $\{\sigma_i\}$ values into Eq. (3) for $|q\rangle$ [now a $(236 + 2)$-component vector] to compute the two sequences' f_{el} and the corresponding phase diagrams. The σ_i's are taken to be constant because we are interested primarily in the physiological and/or experimental pH in
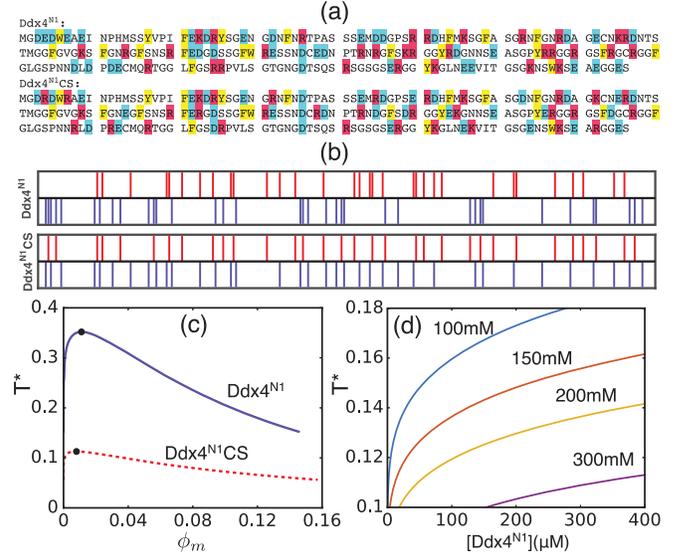
the range of 7.0–8.0 [12], although amino acid charges can change significantly if the pH variation is larger. Comparing the two phase boundaries in the absence of salt ($\rho_s = 0$, but $\rho_c \neq 0$) indicates that charge scrambling leads to an approximately threefold decrease in the critical temperature [Fig. 2(c)], underscoring once again the importance of charge pattern in polyampholyte phase behavior and is in qualitative agreement with the experimental observation that the Ddx4^{N1} phase separates, whereas Ddx4^{N1}CS does not [12]. Interestingly, the predicted ϕ_{cr} of Ddx4^{N1}CS is smaller than that of Ddx4^{N1}, which, according to Fig. 1, suggests that Ddx4^{N1}CS is akin to a sequence with a weaker σ but has longer charge blocks than Ddx4^{N1}. Apparently, the sequential proximity of opposite charges in Ddx4^{N1}CS results in a much weaker effective σ.

We next explore salt effects on the Ddx4^{N1} phase behavior by equating a^3 with the volume of a single water molecule, in which case $\phi_m = 236[Ddx4^{N1}]/55.5$ M because the molarity of water is 55.5. We consider $\phi_s = 0.0018, 0.0027, 0.0036,$ and 0.0054, which are calculated in the same manner, respectively, for [NaCl] $= 100, 150, 200,$ and 300 mM [12]. To compare this with Fig. 4 of Ref. [12], we focus first on the range of [Ddx4^{N1}] $= 0$–400 μM. Figure 2(d) shows a clear decreasing propensity (i.e., requiring a lower T^*) to phase separate with increasing salt. This theoretical salt dependence is expected of Ddx4^{N1} as a nearly neutral

polyampholyte (whereas the phase separation of highly charged polyelectrolytes can be promoted by salt [39]) and is qualitatively consistent with the experiment in Ref. [12].

While Fig. 2(d) provides a conceptual rationalization, it does not match quantitatively with the experimental salt dependence: For $[\text{Ddx4}^{\text{N1}}] \approx 150 \ \mu M$, the ratio of absolute temperatures at the experimental phase boundaries for $[\text{NaCl}] = 100$ and 300 mM is about 1.2 (between $\approx 0\,^{\circ}\text{C}$ and $60\,^{\circ}\text{C}$) [12], but the corresponding theoretical ratio is much higher, at ≈ 1.7. This mismatch means that certain "background" Ddx4 interactions that are less dependent on salt have not been taken into account by our theory. Indeed, aromatic interactions are expected to contribute significantly to the Ddx4 phase properties, as to other IDP behaviors [5,40], because a Ddx4$^{\text{N1}}$ mutant with wild-type charge pattern but with nine of its 14 phenylalanines replaced by alanines does not phase separate [12]. Moreover, repetitive phenylalanine-glycine patterns in IDPs are known to drive phase separation [17,41]. These observations suggest strongly that cation-π and π-π stacking interactions can play central roles in IDP phase separation [12,17,41,42].

With this consideration, we augment our RPA theory for Ddx4$^{\text{N1}}$ with a mean-field account of π interactions, which are known to be spatially short ranged [43,44] and may therefore be formulated, as a first approximation, by a salt-independent FH term,

$$f_{\text{FH}} = \chi \phi_m (1 - \phi_m) = \left(\frac{\varepsilon_h}{T^*} + \varepsilon_s \right) \phi_m (1 - \phi_m), \quad (10)$$

where ε_h and ε_s are the enthalpic and entropic contributions, respectively, to the FH interaction parameter χ. To compare theory with experiment quantitatively, values for the monomer length scale a and the dielectric constant ϵ are needed to convert T^* to the actual temperature. We take a to be the Cα-Cα distance 3.8 Å, and let ϵ be a fitting parameter, as ϵ of an aqueous protein solution can vary widely between ≈ 2 and 80 [45,46]. By treating ε_h and ε_s also as global fitting parameters, a reasonably good fit is achieved with experimental results for all four available $[\text{NaCl}]$ values [12] [Fig. 3(a)] by using a value of $\epsilon = 29.5$ that is physically plausible for a mixture of protein ($\epsilon \approx 2$–4) and water ($\epsilon \approx 80$).

As a self-consistency check, we compare the salt-free phase diagrams of the wild-type and charge-scrambled Ddx4 sequences computed with the augmented FH interaction. Ddx4$^{\text{N1}}$CS is then predicted to never phase separate at temperatures appreciably above $0\,^{\circ}\text{C}$ [Fig. 3(b)], consistent with no observation of Ddx4$^{\text{N1}}$CS phase separation in the experiment under physiological conditions [12]. Our model's ability to rationalize the diverse phase behaviors of Ddx4$^{\text{N1}}$ and Ddx4$^{\text{N1}}$CS simultaneously suggests that it can be applied to predict or rationalize the phase behaviors of other permutations of Ddx4$^{\text{N1}}$ sequences in the future. Interestingly, the ϕ_{cr} of Ddx4$^{\text{N1}}$CS is dramatically shifted from 0.0080 by the FH term to 0.046, which is on the order
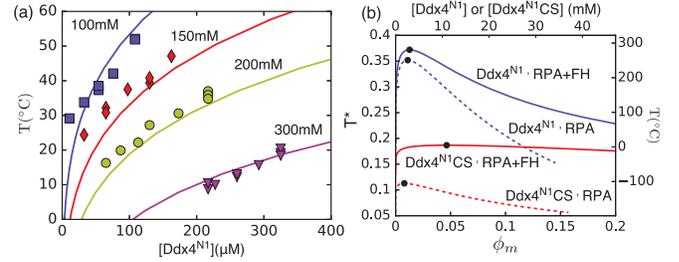

FIG. 3. (a) Theoretical phase diagrams of Ddx4$^{\text{N1}}$ under different $[\text{NaCl}]$ values, computed by RPA theory augmented by FH short-range interactions (the curves), with fitted $\epsilon = 29.5$, $\varepsilon_h = 0.15$, and $\varepsilon_s = -0.3$ (see the text). Experimental data [12] are included for comparison (the symbols; same color code). (b) The salt-free phase diagrams of Ddx4$^{\text{N1}}$ and Ddx4$^{\text{N1}}$CS with and without the FH interaction in Eq. (10).

of the FH critical point $1/\sqrt{236} = 0.065$, indicating that the electrostatic interaction in Ddx4$^{\text{N1}}$CS is weak and its phase behavior is determined mainly by the augmented FH interactions. By contrast, the critical point of the wild-type Ddx4$^{\text{N1}}$ is barely shifted by the augmented FH term, implying that its phase behavior is dominated by electrostatics.

The fitted $\varepsilon_h = 0.15$ and $\varepsilon_s = -0.3$ in Fig. 3 correspond to a favorable enthalpy of $\Delta H = -0.44$ kcal/mol and an unfavorable entropy of $\Delta S = -0.60$ cal/mol K^{-1}. Notwithstanding the limitations of our model, such that part of these augmented FH parameters may be needed to correct for the inaccuracies of the RPA itself, the fitted quantities are in line with our assumption that they should account approximately for favorable π interactions. The cation-π attractive enthalpy between the lysine NH$_4^+$ group and an aromatic ring is about 20 kcal/mol in a gas-phase *ab initio* simulation [43], and, because of the resonant π electron on its guanidinium group [47], the attraction between an arginine and an aromatic ring can be even stronger, though cation-π interaction strength can be weakened in an aqueous environment [48]. Considering there are 32 cations and 22 aromatic rings (14 phenylalanines, 3 tryptophans, and 5 tyrosines) on Ddx4$^{\text{N1}}$ and Ddx4$^{\text{N1}}$CS, the effective ΔH for cation-π interactions in the FH parameter may be estimated to be at least of the order $-20(22 \times 32/236^2) = -0.25$ kcal/mol (note that π-π energies and beyond-pairwise multibody interactions are not included in this estimation), which matches reasonably well with the fitted value. Moreover, formation of cation-π and π-π pairs invariably entails side chain entropy losses, which are consistent with a fitted negative value for ΔS.

We notice that curvature of the phase boundary increases with an increasing ε_h. In view of the experimental trend of decreasing phase-boundary curvature with increasing salt, this observation suggests that the theory-experiment match may be improved by allowing ε_h to decrease slightly with $[\text{NaCl}]$. Such a model may be justifiable because, with increasing salt concentration, aromatic rings are more likely to bind to

surrounding salt cations, rather than engaging with the positively charged lysines and arginines. A detailed analysis of this possibility, however, is beyond the scope of this work.

In summary, we have developed a general analytical theory for sequence-specific electrostatic effects on poly-ampholyte phase separation. Going beyond mean-field theories that do not consider sequence information [12], our theory provides physical underpinnings for experimental Ddx4 behaviors in terms of the charge pattern along its sequence and probable π interactions. Theory and experiment both suggest that an alternating charge pattern that maintains reasonably high average positive or negative charge densities over a length scale encompassing at least several amino acid residues is required for Ddx4 phase separation [12]. It would be instructive to investigate how this principle is manifested in other IDPs. In any event, it would be useful to apply our theory to other IDP poly-ampholytes and to generalize the present formulation to incorporate sequence-specific nonelectrostatic interactions.

---

*Corresponding author.
chan@arrhenius.med.toronto.edu

[1] V. N. Uversky, J. R. Gillespie, and A. L. Fink, Proteins **41**, 415 (2000).

[2] P. Tompa, Trends Biochem. Sci. **37**, 509 (2012).

[3] J. D. Forman-Kay and T. Mittag, Structure **21**, 1492 (2013).

[4] R. van der Lee *et al.*, Chem. Rev. **114**, 6589 (2014).

[5] T. Chen, J. Song, and H. S. Chan, Curr. Opin. Struct. Biol. **30**, 32 (2015).

[6] P. G. Higgs and J.-F. Joanny, J. Chem. Phys. **94**, 1543 (1991).

[7] A. V. Dobrynin, R. H. Colby, and M. Rubinstein, J. Polym. Sci., Part B: Polym. Phys. **42**, 3513 (2004).

[8] C. P. Brangwynne, C. R. Eckmann, D. S. Courson, A. Rybarska, C. Hoege, J. Gharakhani, F. Jülicher, and A. A. Hyman, Science **324**, 1729 (2009).

[9] P. Li, S. Banjade, H.-C. Cheng, S. Kim, B. Chen, L. Guo, M. Llaguno, J. V. Hollingsworth, D. S. King, S. F. Banani, P. S. Russo, Q. Jiang, B. T. Nixon, and M. K. Rosen, Nature (London) **483**, 336 (2012).

[10] M. Kato, T. W. Han, S. Xie, K. Shi, X. Du, L. C. Wu, H. Mirzaei, E. J. Goldsmith, J. Longgood, J. Pei, N. V. Grishin, D. E. Frantz, J. W. Schneider, S. Chen, L. Li, M. R. Sawaya, D. Eisenberg, R. Tycko, and S. L. McKnight, Cell **149**, 753 (2012).

[11] C. F. Lee, C. P. Brangwynne, J. Gharakhani, A. A. Hyman, and F. Jülicher, Phys. Rev. Lett. **111**, 088101 (2013).

[12] T. J. Nott, E. Petsalaki, P. Farber, D. Jervis, E. Fussner, A. Plochowietz, T. D. Craggs, D. P. Bazett-Jones, T. Pawson, J. D. Forman-Kay, and A. J. Baldwin, Mol. Cell **57**, 936 (2015).

[13] M. Dundr and T. Misteli, Cold Spring Harbor Persp. Biol. **2**, a000711 (2010).

[14] J. A. Toretsky and P. E. Wright, J. Cell Biol. **206**, 579 (2014).

[15] A. A. Hyman, C. A. Weber, and F. Jülicher, Annu. Rev. Cell Dev. Biol. **30**, 39 (2014).

[16] S. Elbaum-Garfinkle, Y. Kim, K. Szczepaniak, C. C.-H. Chen, C. R. Eckmann, S. Myong, and C. P. Brangwynne, Proc. Natl. Acad. Sci. U.S.A. **112**, 7189 (2015).

[17] C. P. Brangwynne, P. Tompa, and R. V. Pappu, Nat. Phys. **11**, 899 (2015).

[18] A. H. Mao, S. L. Crick, A. Vitalis, C. L. Chicoine, and R. V. Pappu, Proc. Natl. Acad. Sci. U.S.A. **107**, 8183 (2010).

[19] J. A. Marsh and J. D. Forman-Kay, Biophys. J. **98**, 2383 (2010).

[20] S. Müller-Späth, A. Soranno, V. Hirschfeld, H. Hofmann, S. Rüegger, L. Reymond, D. Nettels, and B. Schuler, Proc. Natl. Acad. Sci. U.S.A. **107**, 14609 (2010).

[21] R. K. Das and R. V. Pappu, Proc. Natl. Acad. Sci. U.S.A. **110**, 13392 (2013).

[22] K. M. Ruff, T. S. Harmon, and R. V. Pappu, J. Chem. Phys. **143**, 243123 (2015).

[23] F. G. Quiroz and A. Chilkoti, Nat. Mater. **14**, 1164 (2015).

[24] P. Gonzalez-Mozuelos and M. O. de la Cruz, J. Chem. Phys. **100**, 507 (1994).

[25] D. W. Cheong and A. Z. Panagiotopoulos, Mol. Phys. **103**, 3031 (2005).

[26] J. Jiang, J. Feng, H. Liu, and Y. Hu, J. Chem. Phys. **124**, 144908 (2006).

[27] L. Liang, W. Diehl-Jones, and P. Lasko, Development (Cambridge, U.K.) **120**, 1201 (1994).

[28] J. Wittmer, A. Johner, and J. F. Joanny, Europhys. Lett. **24**, 263 (1993).

[29] V. Y. Borue and I. Y. Erukhimovich, Macromolecules **21**, 3240 (1988).

[30] K. A. Mahdi and M. Olvera de la Cruz, Macromolecules **33**, 7649 (2000).

[31] A. V. Ermoshkin and M. Olvera de la Cruz, Phys. Rev. Lett. **90**, 125504 (2003).

[32] A. V. Ermoshkin and M. Olvera de la Cruz, J. Polym. Sci., Part B: Polym. Phys. **42**, 766 (2004).

[33] J. Overbeek and M. J. Voorn, J. Cell. Comp. Physiol. **49**, 7 (1957).

[34] A. V. Ermoshkin and M. Olvera de la Cruz, Macromolecules **36**, 7824 (2003).

[35] P. J. Flory, *Principles of Polymer Chemistry* (Cornell University Press, Ithaca, 1953).

[36] P.-G. de Gennes, *Scaling Concepts in Polymer Physics* (Cornell University Press, Ithaca, 1979).

[37] H. S. Chan and K. A. Dill, J. Chem. Phys. **101**, 7007 (1994).

[38] M. Doi and S. F. Edwards, *The Theory of Polymer Dynamics* (Clarendon Press, Oxford, 1986).

[39] A. V. Dobrynin and M. Rubinstein, Prog. Polym. Sci. **30**, 1049 (2005).

[40] J. Song, S. C. Ng, P. Tompa, K. A. W. Lee, and H. S. Chan, PLoS Comput. Biol. **9**, e1003239 (2013).

[41] H. B. Schmidt and D. Görlich, eLife **4**, e04251 (2015).

[42] R. M. Vernon, P. J. Farber, and J. D. Forman-Kay (to be published).

[43] J. C. Ma and D. A. Dougherty, Chem. Rev. **97,** 1303 (1997).

[44] E. A. Meyer, R. K. Castellano, and F. Diederich, Angew. Chem., Int. Ed. Engl. **42,** 1210 (2003).

[45] J. W. Pitera, M. Falta, and W. F. van Gunsteren, Biophys. J. **80,** 2546 (2001).

[46] A. Warshel, P. K. Sharma, M. Kato, and W. W. Parson, Biochim. Biophys. Acta **1764,** 1647 (2006).

[47] S. Marsili, R. Chelli, V. Schettino, and P. Procacci, Phys. Chem. Chem. Phys. **10,** 2673 (2008).

[48] J. P. Gallivan and D. A. Dougherty, Proc. Natl. Acad. Sci. U.S.A. **96,** 9459 (1999).